Physica A 509 (2018) 56–65

Contents lists available at ScienceDirect

Physica A

journal homepage: www.elsevier.com/locate/physa

Early prediction of paroxysmal atrial fibrillation based on short-term heart rate variability

Ali Narin [a], Yalcin Isler [b], Mahmut Ozer [a], Matjaž Perc [c,*]

[a] Bülent Ecevit University, Department of Electrical and Electronics Engineering, Zonguldak, Turkey
[b] Izmir Katip Celebi University, Department of Biomedical Engineering, Cigli, Izmir, Turkey
[c] Faculty of Natural Sciences and Mathematics, University of Maribor, Slovenia

ARTICLE INFO

Article history:
Received 6 June 2018
Available online xxxx

Keywords:
Paroxysmal atrial fibrillation
Heart rate variability
Genetic algorithm
Wavelet packet transform
Early prediction

ABSTRACT

Atrial fibrillation (AF) is the most common arrhythmia type and its early stage is paroxysmal atrial fibrillation (PAF). PAF affects negatively the quality of life by causing dyspnea, chest pain, feeling of excessive fatigue, and dizziness. In this study, our aim is to predict the onset of paroxysmal atrial fibrillation (PAF) events so that patients can take precautions to prevent PAF events. We use an open data from Physionet, Atrial Fibrillation Prediction Database. We construct our approach based on the heart rate variability (HRV) analysis. Short-term HRV analysis requires 5-minute data so that each dataset was divided into 5-minute data segments. HRV features for each segment are calculated from time-domain measures and frequency-domain measures using power spectral density estimations of fast Fourier transform, Lomb–Scargle, and wavelet transform methods. Different combinations of these HRV features are selected by Genetic Algorithm and then applied to *k*-nearest neighbors classification algorithm. We compute the classifier performances by the 10-fold cross-validation method. The proposed approach results in 92% sensitivity, 88% specificity and 90% accuracy in the 2.5–7.5 min time interval priors to PAF event. The proposed method results in better classification performance than the similar studies in literature. Comparing the existing studies, we propose that our approach provide better tool to predict PAF events.

1. Introduction

A healthy heart beats at 60–80 times per minute [1]. Electrical impulses from the sinoatrial (SA) node spread curvaceously to stimulate the atria and initiate contractions for the healthy beat. However, random and multiple impulses are produced in patients with atrial fibrillation (AF), in addition to the impulses from the SA node [2]. These impulses cause fibrillation instead of normal contractions of the atrium.

There are three types of AF: Paroxysmal AF (PAF), Persistent AF, and Chronic AF. PAF is the first-stage of AF. In this situation, AF starts suddenly and continues up to a week. If it is determined as soon as possible, the complications and the progress of this situation can be avoided [3].

AF affects negatively the quality of life by causing dyspnea, chest pain, feeling of excessive fatigue, and dizziness [4,5]. Moreover, AF increases the risk of stroke five times, the risk of death (due to stroke) two times. Consequently, the patient care

* Corresponding author.
E-mail addresses: alinarin45@gmail.com (A. Narin), islerya@yahoo.com (Y. Isler), mahmutozer2002@yahoo.com (M. Ozer), matjaz.perc@uni-mb.si (M. Perc).

https://doi.org/10.1016/j.physa.2018.06.022
0378-4371/

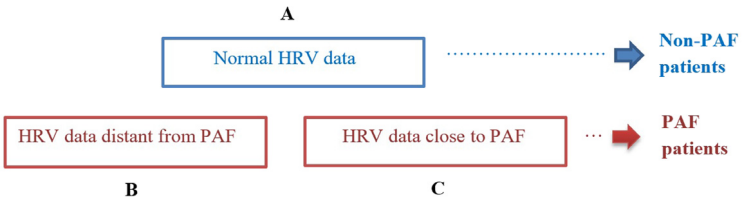

Fig. 1. Datasets used in the study: (A) Normal subjects (B) HRV data distant from PAF (C) HRV data close to PAF.

costs increase 1.5 times [3]. AF is very common among heart diseases with the incidence of 1–2% of the general population. It is estimated that 2.7–6.1 million Americans and over 6 million Europeans suffer from this situation [3,6]. Furthermore, the incidence of AF is around 5–15% at the age of 80s while this is less than 0.5% at the age of 50s, which means the incidence of AF drastically increases by the age [3].

The number of studies related to pre-detection of PAF events has been increased for 2 decades [7–19]. Zong et al. [7] reported that the frequency of APC beats is a highlighting feature before PAF occurs of 30-min ECG signals. Langley et al. [8] have also estimated PAF by looking at the quantities of atrial ectopic and ventricular ectopic beats using 30-min RR data. They have stated that there is a significant increase in atrial ectopic beats before a PAF event [8]. Using 1-min, 5-min, 10-min, and 30-min RR data, Chazal and Henegham [9] have performed early estimation of PAF by using 1–6 correlation coefficients, time-domain measurements, frequency-domain measurements, and *P* waveform and spectral densities, and they found that the power spectral densities and P wave characteristics of RR intervals have distinctive features. In another study, Chesnokov [10] found that the spectral components increase statistically before PAF event while the sample entropy and approximate entropy values decrease. Mohebbi and Ghassemian [11] have used spectral, bispectral and nonlinear measurements obtained from 30-min heart rate variability (HRV) data. Their results indicate that the spectral powers in the LF and HF bands increase before PAF event. In bispectral measurements, phase couplings were observed in data distant from a PAF event, while the phase couplings decrease as the PAF event approaches. They noted that the Poincare measurements might be a critical PAF event indicator [11]. Boon et al. [12,13] investigated the 5-min, 10-min, 15-min, 20-min and 30-min segments of free ectopic data and noted that the performance decreases toward the shorter segments than the 30-min segments.

Another widely used method for predicting PAF in the literature is to examine *P*-wave s on Electrocardiography (ECG) [16–19]. In these studies, researchers have used *P*-wave duration, amplitude, *P*-wave change, spectral power intensities of *P*-wave change and non-linear measurements of *P*-wave. In particular, Alcaraz et al. [17] and Artuno Martinez et al. [18] have shown that *P*-wave is an effective for predicting PAF events beforehand on one-hour data segments.

In this study, we attempt to construct a complex expert system to predict better the onset of the PAF events based on the HRV so that patients can take precautions to prevent PAF events. For this aim, we use a free and open data from Physionet, Atrial Fibrillation Prediction Database (AFPDB). The database contains 30-minute ECG datasets from 49 normal subjects, 25 PAF patients having a PAF event just after recording the data, 25 PAF patients having no immediate experience after recording the data. Each dataset is divided into 5-minute data segments and then HRV features for each segment are calculated from time-domain measures and frequency-domain measures using power spectral density estimations of fast Fourier transform, Lomb–Scargle, and wavelet transform methods. Different combinations of these HRV features are selected by Genetic Algorithm (GA) and then applied to *k*-nearest Neighbors classification algorithm. Then, we compute the classifier performances by the 10-fold cross-validation method.

2. Materials and methods

2.1. Data

We use the Atrial Fibrillation Prediction Database (AFPDB), which is free and open to all researchers on Phsionet.org website [20]. All ECG datasets in the database are sampled by the sampling rate of 128 Hz, digitized by a resolution of 12 bits and included 30-minute ECG records. The database consists of two parts: 50 datasets from normal subjects and 50 datasets from patients with PAF. The PAF datasets are also divided into two parts: (1) 25 data just before a PAF event and (2) 25 data with no PAF events 45 min before or after the recording. The general representation of the data is given in Fig. 1.

Nonetheless, the dataset numbered 'n27' among normal datasets is excluded from the study because it has excessive noise. This case has been reported in similar studies [21]. As a result, in this study, 49 datasets from normal subjects, 25 datasets from PAF patients with an event and 25 datasets from PAF patients with no near event are included.

2.1.1. Data segmentation

Standards of HRV analysis were determined by the Task Force group in 1996, a 5-minute recording period is recommended for short-term HRV analysis and a 24-hour recording period is recommended for long-term HRV analysis [22]. In order to determine more precise time before the PAF event, short-term (5-minute) HRV analysis is preferred. Based on this approach, all 30-min segments of data were divided into 10 5-minute segments with 50% overlap as shown in Fig. 2.

For all the HRV data segments, we calculate the HRV features and the classifier performances.

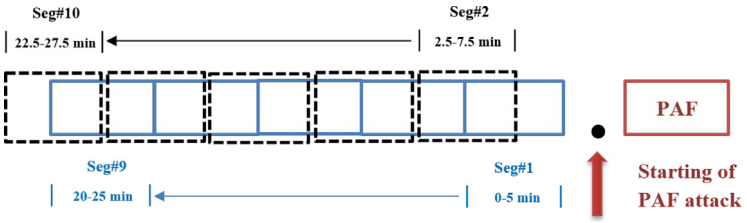

Fig. 2. Representation of HRV data divided into 10 parts of 5 min.

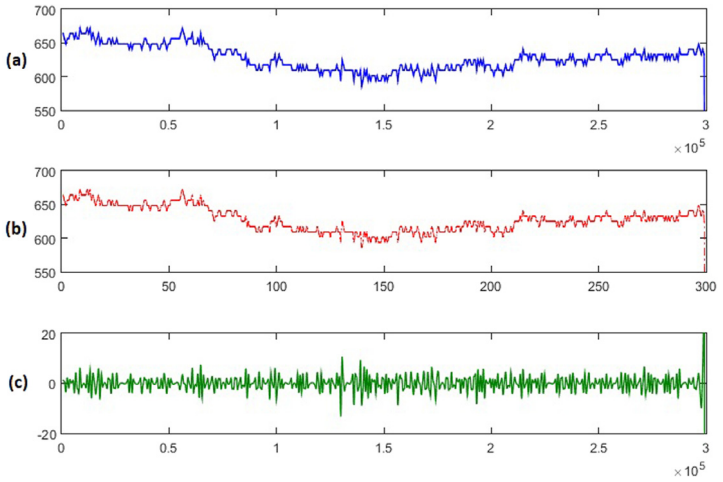

Fig. 3. An example of HRV signal: (a) Original HRV signal (b) Signal after the cubic spline method (c) Signal without a trend.

2.1.2. Data pre-processing

HRV data is an unevenly sampled data and contains non-stationary components and noises [22]. Some feature extraction methods require evenly sampled data (FFT & Wavelet) and/or free of non-stationary components (FFT). In order to make the data evenly sampled one, a re-sampling (interpolation) method should be used. Since the upper-frequency limit of HRV data is defined as 0.5 Hz, the HRV data can be resampled with the sampling rate of 1 to 10 Hz in the literature [23]. In some frontier studies, it has been argued that the appropriate sampling frequency is 4 Hz or 7 Hz [23,24]. The resampling frequency was chosen as 7 Hz in this study. We prefer the Cubic Spline method because it is widely used due to its continuity and smooth transitions [25,26].

HRV data have a non-stationary structure that has linear or more complex trends. Since these trends are very influential in HRV measurements, these trends should be eliminated [23,27] or discarded [28]. The Smoothness Priors method is a popular method among the most common de-trending methods. Researchers prefer this method because it can be used on HRV data [27], its Matlab code is readily available, and it is easy to use. Using the second-order derivative expressions, the stationary data are expressed as follows:

$$x_{stationary} = x - H\hat{\theta}_{\lambda} = \left(I - \left(I + \lambda D_2^T D_2\right)^{-1}\right) x \tag{1}$$

where x is HRV data, D_2 is the second order difference operator, λ is the regulatory parameter ($\lambda = 10$), and $x_{stationary}$ is the signal without trends. A detailed information about this method can be found in [28]. An example HRV data, its trend component and stationary signal are shown in Fig. 3.

2.2. The HRV analysis

The HRV analysis has become a very popular method for researchers. It has been used in the diagnosis of many diseases and the description of the functions of the autonomic nervous system and cardiovascular systems [29–34]. HRV features are calculated from time-domain, frequency-domain, and nonlinear measurements. Each feature vector is expressed as a dimension, which forms a d-dimensional feature space. All of the features obtained from the 5-minute segments of data are defined briefly below.

2.2.1. The HRV time-domain features

HRV time-domain features allow data to be examined statistically. It is the easiest method among the HRV measurements [24,35]. The HRV time-domain features are defined as follows [22]:

AVNN (or ***RR***) is the average HRV value; SDNN is the standard deviation of the HRV data; SDSD is the standard deviation of the differences of consecutive HRV data; RMSSD is the root mean square value of consecutive HRV data; NN50 is the total number of consecutive HRV data differences greater than 50 ms; NN20 is the total number of consecutive HRV data differences greater than 20 ms; pNN50 is the ratio of NN50 value; and pNN20 is the ratio of NN20 value.

2.2.2. The HRV frequency-domain features

Different frequency components in the HRV indicate both sympathetic and parasympathetic changes in the autonomic nervous system. In the literature related to short-term HRV analysis, there are three frequency bands: very low frequency (VLF) (0–0.04 Hz), low frequency (LF) (0.04–0.15 Hz) and high frequency (HF) (0.15–0.40 Hz) [22]. In the long-term HRV analysis, there is an extra ultra-low frequency band (ULF) (0–0.0033 Hz) and the lower limit of VLF is changed to 0.0033 Hz. In HRV analysis, power spectral density (PSD) of these frequency bands are used as possible features. We use three alternatives for determining the frequency-domain features: Fast Fourier Transform, Lomb and Wavelet-based approaches.

2.2.2.1. Fast Fourier Transform. Fast Fourier transform (FFT) is a fast and efficient method to calculate the discrete Fourier transform (DFT). The DFT of the x signal, which is sampled at N equally spaced intervals and its time-domain mean and variance do not change during the time, can be found at:

$$X(k) = \sum_{n=0}^{N-1} \left(x(n)\, e^{\frac{-j2\pi kn}{N}} \right) \tag{2}$$

$k = 0, \mp 1, \mp 2, \ldots, \mp (N-1)$.

The direct calculation of DFT increases the number of operations too much if the N sequence length in the equation is high. A solution to this problem is the Fast Fourier Transform (FFT) method, which makes the calculation faster and yields the same result [36]. Power spectral density can be calculated as:

$$P_x = \frac{1}{N} \sum_{k=0}^{N-1} |X(k)|^2 = \frac{1}{N} \sum_{k=0}^{N-1} \left| \sum_{n=0}^{N-1} \left(x(n)\, e^{\frac{-j2\pi kn}{N}} \right) \right|^2 \tag{3}$$

where $X(k)$ values are selected to the corresponding frequency band. Because of the requirements of the method, x must be an evenly-sampled and stationary signal. Therefore, resampled and detrended HRV data can be used in calculating PSD using FFT.

2.2.2.2. Lomb–Scargle Periodogram. The Lomb–Scargle Periodogram (LS) is a method of calculating the PSD without the need for resampling and eliminating trends [24,37–39]. The LS algorithm was found by Lomb [37] and improved by Scargle [38] as follows:

$$P(w) = \frac{1}{2\sigma^2} \left\{ \frac{\left[\sum_{i=0}^{N-1} \left(x_i - \acute{x} \right) \cos\left(w\left(t_i - \tau \right) \right) \right]^2}{\sum_{i=0}^{N-1} \cos^2\left(w\left(t_i - \tau \right) \right)} + \frac{\left[\sum_{i=0}^{N-1} \left(x_i - \acute{x} \right) \sin\left(w\left(t_i - \tau \right) \right) \right]^2}{\sum_{i=0}^{N-1} \sin^2\left(w\left(t_i - \tau \right) \right)} \right\} \tag{4}$$

$$\tau \equiv \frac{1}{2w} \tan^{-1} \left(\frac{\sum_{i=1}^{N} \sin(w t_i)}{\sum_{i=1}^{N} \cos(w t_i)} \right) \tag{5}$$

where $w = 2\pi f$, τ is the offset value, x is the signal to which the method is applied, $\acute{x}$ is the mean value of the signal, t_i is the ith sampling time, σ^2 is the variance value of the samples.

Scargle [39] has proved that the resultant periodogram values have the same probability distribution as the uniformly distributed data. The Fourier Transform and the Lomb algorithm give similar results when tested both numerically and theoretically.

2.2.2.3. Wavelet packet transform. The wavelet transform is an appropriate method for non-stationary signals, which allows analysis of the sudden changes in the spectrum [40,41]. All sub packages are applied to the algorithm in the wavelet packet transform and only low-frequency packages are applied to the algorithm in the discrete wavelet transform. The wavelet packet transform (WPT) gives a more detailed analysis of high-frequency components of the signal.

The choice of the mother wavelet function is important in wavelet transforms. Daubechies wavelet functions give better results on ECG and HRV signals [29,42]. Therefore, in this study, 7-level wavelet packet transformations are obtained by using Daubechies 4 wavelet function.

Table 1
Confusion matrix.

		Actual value	
		Near PAF event	No near-PAF event
Predicted value	Near PAF event	TP True positive	FP False positive
	No near-PAF event	FN False negative	TN True negative

Table 2
Grouping of data.

CLASS	Group 1	Group 2
Positive	Experienced PAF event	Experienced PAF event
Negative	Did not experience PAF event+ Normal subjects	Did not experience PAF event

Table 3
k-NN performance results for Time + FFT measurements. Group 1 includes all subjects including normal subjects and patients with PAF where Group 2 includes only patients with PAF.

Segments	Group 1						Group 2					
(min)	*k*	SEN (%)	SPE (%)	NEG (%)	POS (%)	ACC (%)	*k*	SEN (%)	SPE (%)	NEG (%)	POS (%)	ACC (%)
0.0–5.0	17	12.0	100	77.1	100	77.8	7	64.0	76.0	67.9	72.7	70.0
2.5–7.5	**5**	**44.0**	**95.9**	**83.5**	**76.6**	**82.8**	5	56.0	84.0	65.6	77.8	70.0
5.0–10.0	3	44.0	91.9	82.9	64.7	79.8	**3**	**60.0**	**84.0**	**67.7**	**78.9**	**72.0**
7.5–12.5	13	8.0	100	76.3	100	76.8	7	72.0	52.0	65.0	60.0	62.0
10.0–15.0	7	40.0	93.2	82.1	66.7	79.8	11	76.0	60.0	71.4	65.5	68.0
12.5–17.5	11	12.0	97.3	76.6	60.0	75.8	11	56.0	68.0	60.7	63.6	62.0
15.0–20.0	13	12.0	100	77.1	100	77.8	9	64.0	68.0	65.4	66.7	66.0
17.5–22.5	13	24.0	90.3	79.1	75.0	78.8	13	64.0	56.0	60.9	59.3	60.0
20.0–25.0	11	8.0	98.6	76.0	66.7	75.8	1	64.0	64.0	64.0	64.0	64.0
22.5–27.5	17	4.0	100	75.5	100	75.8	19	76.0	36.0	60.0	54.3	56.0

It is a frequently used measure of wavelet entropy calculation in wavelet transforms [43,44]. The calculation of wavelet entropy is as follows

$$W_{ENTROPY} = -\sum_{j\in f}\left(\frac{C_j^2}{\sum_{j=1}^{N} C_j^2}\log_2\left(\frac{C_j^2}{\sum_{j=1}^{N} C_j^2}\right)\right) \tag{6}$$

where C_j denotes the jth coefficient of the last wavelet level.

2.3. Feature selection

Some of the features have a negative effect on the classifier performance to discriminate classes, which is called curse-of-dimensionality [45]. A feature selection method is applied to avoid this effect and to find the best representative features [46]. In this study, we use the genetic algorithm (GA) for the future selection.

The GA is an optimization method based on fundamentals of the reproduction of generations and the survival of individuals. In the GA, variables are converted to a sequence of a certain-length binary sequence. Every bit in GA expresses the corresponding feature. For example, if the bit is "1" at the kth bit, that feature is included in the study. If it is "0", this feature will not be included in the study. The fitness function is the most important part of the GA because new individuals are formed based on this function, and defined as follows [47]:

$$Fitness\ Function = FN + FP \tag{7}$$

where FN is the number of misclassified PAF-event subjects as non-PAF-event subjects and FP is the number of misclassified non-PAF-event subjects as PAF-event subjects in the classifier.

2.4. k-nearest neighbor classifier

The k-nearest neighbor is one of the simplest classifiers among many classifier algorithms in data mining. This classifier does not need a training phase and the data is stored only. While classifying the test data, the datum is assigned to the class of the majority class of k-nearest neighbors [45]. The distances between the test sample and all stored samples are sorted in an ascending order and the neighborhoods are determined. The most commonly used distance measure is Euclidean distance defined as follows:

$$D(x, y) = \sqrt{\sum_{k=1}^{n}(x_k - y_k)^2} \tag{8}$$

Table 4
k-NN performance results for Time + FFT + GA. Group 1 includes all subjects including normal subjects and patients with PAF where Group 2 includes only patients with PAF.

Segments (min)	Group 1							Group 2						
	k	SEN (%)	SPE (%)	NEG (%)	POS (%)	ACC (%)	Selected features	*k*	SEN (%)	SPE (%)	NEG (%)	POS (%)	ACC (%)	Selected features
0.0–5.0	**1**	**64.0**	**90.5**	**88.2**	**69.6**	**83.8**	**RMSSD, NN20, pNN20, FFT_VLF, FFT_HF**	3	**92.0**	**88.0**	**91.7**	**88.5**	**90.0**	**RMSSD, FFT_VLF, F FT_LF, FFT_TOTAL**
2.5–7.5	5	44.0	95.9	83.5	78.6	82.8	Mean, RMSSD, HH50, NN20, FFT_LF/HF, FFT_TOTAL	5	72.0	92.0	76.7	90.0	82.0	SDNN, pNN20, FFT_LF, FFT_HF, FFT_TOTAL
5.0–10.0	**5**	**52.0**	**94.6**	**85.4**	**76.5**	**83.8**	**Mean, SDNN, RMSSD, NN20, FFT_VLF, FFT_LF, FFT_LF/HF**	5	76.0	76.0	76.0	76.0	76.0	SDNN, RMSSD, NN20, FFT_HF, FFT_TOTAL
7.5–12.5	5	28.0	95.9	79.8	70.0	78.8	Mean, SDSD, NN50, pNN50, pNN20	5	68.0	64.0	66.7	65.4	66.0	Mean, SDNN, FFT_LF, FFT_HF
10.0–15.0	3	56.0	90.5	85.9	66.7	81.8	SDNN, RMSSD, pNN20, FFT_VLF, FFT_LF, FFT_TOTAL	13	64.0	80.0	69.0	76.2	72.0	SDNN, RMSSD, FFT_VLF, FFT_TOTAL
12.5–17.5	3	44.0	91.9	82.9	64.7	79.8	SDNN, pNN20, FFT_VLF, FFT_LF, FFT_HF, FFT_LF/HF, FFT_TOTAL	13	72.0	56.0	66.7	62.0	64.0	Mean, SDNN, RMSSD, FFT_HF
15.0–20.0	15	12.0	98.6	76.8	75.0	76.8	NN50, NN20, pNN20, FFT_VLF	3	60.0	80.0	66.7	75.0	70.0	SDNN, RMSSD, FFT_VLF, FFT_HF
17.5–22.5	11	24.0	98.6	79.3	85.7	79.8	SDNN, NN50, pNN50, pNN20, FFT_VLF, FFT_LF, FFT_HF	9	72.0	52.0	65.0	60.0	62.0	SDNN, RMSSD, NN50, NN20, pNN20, FFT_VLF, FFT_LF, FFT_TOTAL
20.0–25.0	11	32.0	97.3	80.9	80.0	80.8	NN20, pNN50, pNN20, FFT_LF, FFT_TOTAL	3	76.0	60.0	71.4	65.5	68.0	SDNN, NN50, NN20, pNN50
22.5–27.5	5	28.0	94.6	79.5	63.6	77.8	Mean, NN50, FFT_VLF, FFT_LF, FFT_HF	5	68.0	52.0	61.9	58.6	60.0	SDNN, RMSSD, FFT_HF, FFT_TOTAL

Table 5
k-NN performance results for Time + LOMB measurements (NaN: there is no value). Group 1 includes all subjects including normal subjects and patients with PAF where Group 2 includes only patients with PAF.

Segments (min)	Group 1						Group 2					
	k	SEN (%)	SPE (%)	NEG (%)	POS (%)	ACC (%)	*k*	SEN (%)	SPE (%)	NEG (%)	POS (%)	ACC (%)
0.0–5.0	7	12.0	98.6	76.8	75.0	76.8	**9**	**64.0**	**76.0**	**67.9**	**72.7**	**70.0**
2.5–7.5	**5**	**28.0**	**98.6**	**80.2**	**87.3**	**80.8**	**7**	**56.0**	**84.0**	**65.6**	**77.8**	**70.0**
5.0–10.0	15	16.0	100	77.9	100	78.8	9	56.0	76.0	63.3	70.0	66.0
7.5–12.5	11	0.0	100	74.7	NaN	74.7	15	52.0	76.0	61.0	68.4	64.0
10.0–15.0	7	24.0	94.6	78.7	60.0	76.8	9	64.0	64.0	64.0	64.0	64.0
12.5–17.5	7	16.0	94.6	76.9	50.0	74.7	7	72.0	60.0	67.2	64.3	66.0
15.0–20.0	11	4.0	100	75.5	100	75.8	15	44.0	80.0	58.8	68.8	62.0
17.5–22.5	13	12.0	98.6	66.8	75.0	76.8	1	52.0	72.0	60.0	65.0	62.0
20.0–25.0	13	4.0	100	75.5	100	75.8	1	64.0	64.0	64.0	64.0	64.0
22.5–27.5	7	20.0	98.6	78.5	83.3	78.8	3	48.0	72.0	58.1	63.2	60.0

2.5. The classifier performance

In order to compute the classifier performance, data are divided into test and train clusters using the cross-validation methods of the holdout, the *k*-fold, the re-substitution, or the leave-one-out. In this study, we compute the classifier performance by using the *k*-fold cross-validation method, where the data are divided into *k* parts, one of these parts is used for testing while the remaining $k-1$ parts are used for training. The values of TP, TN, FP, and FN are computed as shown in Table 1. This process is repeated *k* times to determine overall values of TP, TN, FP, and FN [45]. where TP is the number of subjects who actually have a near PAF event and determined correctly, FN is the number of subjects who actually have a near PAF event but misclassified as no near PAF event, TN is the number of subjects who actually do not have a near-PAF event and determined correctly, and FP is the number of subjects who actually do not have a near-PAF event but misclassified as near-PAF event. After computing these values, performance measures of sensitivity (SEN), specificity (SPE), positive predictivity (POS), negative predictivity (NEG), and accuracy (ACC) can be calculated as follows:

$$SEN = \frac{TP}{TP + FN} \tag{9}$$

$$SPE = \frac{TN}{TN + FP} \tag{10}$$

$$NEG = \frac{TN}{TN + FN} \tag{11}$$

$$POS = \frac{TP}{TP + FP} \tag{12}$$

Table 6
k-NN performance results for Time + LOMB + GA. Group 1 includes all subjects including normal subjects and patients with PAF where Group 2 includes only patients with PAF.

Segments (min)	Group 1							Group 2						
	k	SEN (%)	SPE (%)	NEG (%)	POS (%)	ACC (%)	Selected features	*k*	SEN (%)	SPE (%)	NEG (%)	POS (%)	ACC (%)	Selected features
0.0–5.0	**1**	**64.0**	**90.5**	**88.2**	**69.6**	**83.8**	**RMSSD, pNN20, LOMB_LF, LOMB_HF, LOMB_LF/HF**	**5**	**84.0**	**88.0**	**84.6**	**87.5**	**86.0**	**SDNN, RMSSD, LOMB_LF/HF**
2.5–7.5	7	36.0	97.3	81.8	81.8	81.8	Mean, SDNN, RMSSD, SDSD, NN50, NN20, pNN50, pNN20, LOMB_HF, LOMB_LF/HF	3	76.0	88.0	78.6	86.4	82.0	SDNN, pNN20, LOMB_VLF
5.0–10.0	15	24.0	97.3	79.1	75.0	79.1	Mean, SDNN, RMSSD, SDSD, LOMB_HF, LOMB_LF/HF	5	64.0	84.0	70.0	80.0	74.0	SDNN, RMSSD, pNN20, LOMB_HF
7.5–12.5	5	32.0	94.6	80.5	66.7	80.5	Mean, RMSSD, SDSD, pNN20	11	68.0	68.0	68.0	68.0	68.0	LOMB_HF
10.0–15.0	7	24.0	98.6	79.3	85.7	79.8	NN50, pNN50, LOMB_LF	9	68.0	76.0	70.4	73.9	72.0	SDNN
12.5–17.5	5	32.0	93.2	80.2	61.5	77.8	RMSSD, NN50, NN20, pNN20, LOMB_HF, LOMB_LF/HF	3	48.0	88.0	62.9	80.0	68.0	LOMB_LF, LOMB_HF
15.0–20.0	15	20.0	97.3	78.3	71.4	77.8	SDNN, RMSSD, NN50, pNN50, pNN20, LOMB_HF, LOMB_LF/HF	1	68.0	76.0	70.4	73.9	72.0	SDSD, LOMB_LF/HF
17.5–22.5	5	20.0	97.3	78.3	71.4	77.8	Mean	3	76.0	60.0	71.4	65.5	68.0	SDNN, NN50, pNN50, pNN20, LOMB_HF, LOMB_LF/HF
20.0–25.0	5	32.0	95.9	80.7	72.7	79.8	SDNN, NN20, LOMB_HF, LOMB_LF/HF	3	64.0	80.0	69.0	76.2	72.0	RMSSD, NN20, LOMB_HF, LOMB_LF/HF
22.5–27.5	7	40.0	95.9	82.6	76.9	81.8	SDNN, LOMB_VLF, LOMB_HF, LOMB_LF/HF	3	72.0	60.0	68.2	64.3	66.0	SDNN, LOMB_LF, LOMB_HF, LOMB_LF/HF, LOMB_TOTAL

Table 7
k-NN performance results for Time + Wavelet measurements. Group 1 includes all subjects including normal subjects and patients with PAF where Group 2 includes only patients with PAF.

Segments (min)	Group 1						Group 2					
	k	SEN (%)	SPE (%)	NEG (%)	POS (%)	ACC (%)	*k*	SEN (%)	SPE (%)	NEG (%)	POS (%)	ACC (%)
0.0–5.0	**13**	**36.0**	**95.9**	**81.6**	**75.0**	**80.8**	7	64.0	80.0	69.0	76.2	72.0
2.5–7.5	3	44.0	91.9	82.9	64.7	79.8	9	52.0	88.0	64.7	81.3	70.0
5.0–10.0	5	36.0	91.9	81.0	60.0	77.8	**9**	**76.0**	**72.0**	**75.0**	**73.1**	**74.0**
7.5–12.5	5	4.0	100	75.5	100	75.8	19	88.0	36.0	75.0	57.9	62.0
10.0–15.0	3	40.0	87.8	81.3	52.6	75.8	13	52.0	52.0	52.0	52.0	62.0
12.5–17.5	11	4.0	100	75.5	100	75.8	3	52.0	64.0	57.1	59.1	58.0
15.0–20.0	13	8.0	98.6	76.0	66.7	75.8	7	68.0	52.0	61.9	58.6	60.0
17.5–22.5	9	20.0	97.2	78.3	71.4	77.8	1	60.0	72.0	64.3	68.2	66.0
20.0–25.0	7	20.0	95.9	78.0	62.5	76.8	13	84.0	40.0	71.4	58.5	62.0
22.5–27.5	9	4.0	100	75.5	100	75.8	9	72.0	52.0	65.0	60.0	62.0

$$ACC = \frac{TP + TN}{TP + FN + FP + TN} \tag{13}$$

3. Results and discussion

In this study, AFPDB data obtained from Physionet website (which contains ECG datasets from 49 normal subjects, 25 patients having following PAF event and 25 patients having no near PAF event) were used to predict a PAF event before its onset. Short-term (5-minute) HRV analysis is used to calculate time-domain measures (8 features) and frequency-domain measures (18 features) for 10 time-segments. Using these features, we investigated which 5-min segment (or segments) can indicate a possible near PAF event.

For this purpose, we tried to find out answers for two questions: "how many minutes before a PAF event were required to predict among all normal subjects and patients with PAF?" as a first question (Group 1) and "how many minutes before a PAF event were required to predict among all patients with PAF?" as a second question (Group 2) as shown in Table 2. For this purpose, GA selects the combinations of 5-minute HRV features of time-domain and frequency-domain measures and applies to the inputs of the *k*-nearest Neighbors classifier. Datasets used in the study divided into 10 time-segments of 5-minute HRV data. The neighborhood value of *k* was applied as odd numbers from 1 to 19. As a result, the study was repeated 10 (time-segments) × 2 (groups) × 10 ($k = 1, 3, 5, \ldots, 19$) × 2 (apply all features and only selected features by GA) × 3 (feature combinations of Time + FFT, Time + Lomb, Time + Wavelet) = 1200 times and classifier performances were recorded.

For each 5-minute data segment, the following 26 HRV time-domain and frequency-domain features were computed separately: MEAN, SDNN, RMSSD, SDSD, NN50, NN20, pNN50, pNN20, FFT_VLF, FFT_LF, FFT_HF, FFT_LF/HF, FFT_TOTAL, LOMB_VLF, LOMB_LF, LOMB_HF, LOMB_LF/HF, LOMB_TOTAL, Wave_VLF, Wave_LF, Wave_HF, Wave_LF/HF, Wave_TOTAL, Ent_VLF, Ent_LF, and Ent_HF.

Table 8
k-NN performance results for Time + Wavelet + GA. Group 1 includes all subjects including normal subjects and patients with PAF where Group 2 includes only patients with PAF.

Segments (min)	Group 1							Group 2						
	k	SEN (%)	SPE (%)	NEG (%)	POS (%)	ACC (%)	Selected features	*k*	SEN (%)	SPE (%)	NEG (%)	POS (%)	ACC (%)	Selected features
0.0–5.0	**7**	**64.0**	**87.8**	**87.8**	**64.0**	**81.8**	**SDNN, RMSSD, Wave_HF, Wave_TOTAL, Ent_LF**	**1**	**84.0**	**84.0**	**84.0**	**84.0**	**84.0**	**SDNN, NN50**
2.5–7.5	**7**	**36.0**	**97.3**	**81.8**	**81.8**	**81.8**	**Mean, SDNN, RMSSD, pNN50, pNN20, Wave_LF, Wave_TOTAL, Ent_HF**	3	72.0	88.0	75.6	85.7	80.0	SDNN, RMSSD, pNN20, Wave_TOTAL
5.0–10.0	13	48.0	91.9	84.0	66.7	80.8	Mean, SDNN, RMSSD, Wave_HF, Wave_LF/HF, Wave_TOTAL	5	80.0	72.0	78.3	74.1	76.0	SDNN, Wave_VLF, Wave_HF, Wave_LF/HF, Ent_LF, Ent_HF
7.5–12.5	5	32.0	94.6	80.5	66.7	78.8	Mean, RMSSD, SDSD, pNN20, Wave_VLF	3	84.0	64.0	80.0	70.0	74.0	NN20, pNN50, Wave_LF/HF
10.0–15.0	11	12.0	98.6	76.8	75.0	76.8	RMSSD, NN20, pNN50, Wave_VLF, Wave_LF, Ent_LF	7	72.0	76.0	73.1	75.0	74.0	SDNN, Ent_HF
12.5–17.5	1	52.0	86.5	84.2	56.5	77.8	NN20, pNN20, Ent_VLF, Ent_LF, Ent_HF	1	60.0	68.0	63.0	65.2	64.0	SDSD, NN20, pNN50, Wave_LF, Wave_LF/HF, Ent_VLF
15.0–20.0	3	48.0	89.2	83.5	60.0	78.8	SDNN, NN50, NN20, pNN20, Wave_LF/HF, Ent_LF, Ent_HF	9	76.0	60.0	71.4	65.5	68.0	SDNN, RMSSD, Wave_VLF, Wave_HF, Ent_VLF, Ent_LF
17.5–22.5	9	16.0	100	77.9	100	78.7	RMSSD, NN50, NN20, Wave_LF, Wave_HF, Wave_TOTAL, Ent_LF, Ent_HF	1	72.0	72.0	72.0	72.0	72.0	SDNN, RMSSD, pNN20, Wave_VLF, Wave_LF, Ent_VLF, Ent_HF
20.0–25.0	9	40.0	94.6	82.4	71.4	80.8	RMSSD, NN50, Wave_HF, Wave_TOTAL	5	64.0	76.0	67.9	72.7	70.0	RMSSD, NN50, pNN50, Wave_LF, Wave_HF, Wave_TOTAL, Ent_VLF, Ent_HF
22.5–27.5	9	4.0	100	75.5	100	75.8	SDSD, pNN50, Wave_LF, Wave_HF, Wave_LF/HF, Wave_TOTAL	15	84.0	40.0	71.4	58.3	62.0	RMSSD, NN50, pNN50, Wave_VLF, Wave_LF, Ent_VLF

Table 9
Literature review.

Literature	Database	Data length (min)	Features	Cross-validation	Results (%)		
					SEN	SPE	ACC
Chazal and Henegham [9]	AFPDB	10	RR interval FFT power spectral density	5-fold	91.0	84.0	86.8
	AFPDB	10	RR interval time domain measures	5-fold	90.0	59.0	77.6
	AFPDB	**5**	***P*-wave power spectral density**	**5-fold**	**81.0**	**69.0**	**75.6**
Hickey and Henegham [48]	AFPDB	30	**HRV power spectral density and PACs**	5-fold	79.0	72.0	75.0
	AFPDB	**5**		**5-fold**	**51.0**	**79.0**	**68.0**
Zong et al. [7]	AFPDB	30	Number and timing of PACs	Single-fold	–	–	80.0
Thong et al. [49]	AFPDB	30	Number of PACs and paroxysmal atrial tachycardia	Single-fold	68.0	86.0	78.0
Chesnokov [10]	AFPDB	30	HRV features	Single-fold	68.2	100	82.0
	AFPDB	30		Single-fold	83.7	76.5	80.5
	AFPDB	30		Single-fold	79.1	58.8	70.1
Mohebbi and Ghassemain [11]	AFPDB	30	HRV features	Single-fold	96.3	93.1	94.6
Boon et al. [12]	AFPDB	30	HRV features	Single-fold	96.4	71.4	83.9
	AFPDB	30		10-fold	81.1	79.3	80.2
	AFPDB	10		Single-Fold	75.1	54.3	69.6
	AFPDB	10		10-fold	58.5	81.1	68.9
	AFPDB	15		Single-fold	85.1	82.1	83.9
	AFPDB	15		10-fold	77.4	81.1	79.3
Boon et al. [13]	**AFPDB**	**5**	**HRV features**	**10-fold**	**86.8**	**88.7**	**87.7**
Martinez et al. [18]	Own data	60	*P*-wave nonlinear features	2-fold	92.0	88.0	90.0
Alcaraz et al. [17]	Own data	60	*P*-wave spectral features	2-fold	–	–	88.0
This Study	**AFPDB**	**5**	**HRV linear and nonlinear features combination**	**10-fold**	**92.0**	**88.0**	**90.0**

We first computed the classifier performances with both HRV time-domain and HRV FFT-based frequency-domain features. The obtained results are shown in Table 3. We also computed the classifier performances with some selected features of both HRV time-domain and HRV FFT-based frequency-domain features by GA, and shown in Table 4. The highest accuracies are obtained as 82.8% for Group 1 and 72.0% for Group 2 when all features are considered for the classifier. On the other hand, the highest accuracies are obtained as 83.8% for Group 1 and 90.0% for Group 2 when only selected features are applied to the classifier. Feature selection by GA increases the classifier performances.

Secondly, we computed the classifier performances with both HRV time-domain and HRV Lomb-based frequency-domain features. The obtained results are shown in Table 5. We also computed the classifier performances with some selected features of both HRV time-domain and HRV Lomb-based frequency-domain features by GA, and shown in Table 6. The highest accuracies are obtained as 80.8% for Group 1 and 70.0% for Group 2 when all features are considered for the classifier. On the other hand, the highest accuracies are obtained as 83.8% for Group 1 and 86.0% for Group 2 when only selected features

are applied to the classifier. Results indicate that the feature selection by GA plays critical role by increasing the classifier performances.

Finally, we computed the classifier performances with both HRV time-domain and HRV Wavelet-based frequency-domain features. The obtained results are shown in Table 7. We also computed the classifier performances with some selected features of both HRV time-domain and HRV Wavelet-based frequency-domain features by GA, and shown in Table 8. The highest accuracies are obtained as 80.8% for Group 1 and 74.0% for Group 2 when all features are considered for the classifier. On the other hand, the highest accuracies are obtained as 81.8% for Group 1 and 84.0% for Group 2 when only selected features are applied to the classifier. Results again indicate that the feature selection by GA plays critical role by increasing the classifier performances.

As mentioned above, we used three alternatives for determining the frequency-domain features through FFT, Lomb and Wavelet-based approaches. We reached at the best classifier performance with an accuracy of 90%, specificity of 88% and sensitivity of 92% for the FFT-based approach.

We summarized the current literature in Table 9. It seems that there are three separate studies by using the 5-min segments. Chazal and Henegham [9] used AFPDB database and obtained a classification performance of an accuracy of 75,6%, specificity of 69,0% and sensitivity of 81% by using *P*-wave power spectral density. Hickey and Henegham [48] used the same database and reached at a classification performance of an accuracy of 68%, specificity of 79,0% and sensitivity of 51% by using HRV power spectral density and PACs. In a very recent study, Boon et al. [13] reconsidered the issue by using 5-min HRV segments and obtained a performance in classification with an accuracy of 87,7%, specificity of 88,7% and sensitivity of 86,8%. Consequently, the proposed method in this study results in better classification performance than the similar studies in literature. We may propose that our approach provide better tool to predict PAF events.

References

[1] J.E.P. Waktare, Cardiology patient page-atrial fibrillation, Circulation 106 (2002) 14–16.
[2] S. Nattel, New ideas about atrial fibrillation 50 years on, Nature 415 (2002) 219–226.
[3] A.J. Camm, P. Kirchhof, G.Y. Lip, U. Schotten, I. Savelieva, S. Ernst, et al., Guidelines for the management of atrial fibrillation the task force for the management of atrial fibrillation of the European Society of Cardiology, ESC, Eur. Heart J. 31 (2010) 2369–2429.
[4] M. Rienstra, S.A. Lubitz, S. Mahida, et al., Symptoms and functional status of patients with atrial fibrillation, Circulation 125 (23) (2012) 2933–2943.
[5] W.S. Aronow, Management of the older person with atrial fibrillation, J. Gerontol. (A Biol. Sci. Med. Sci.) 57 (6) (2002) 352–363.
[6] C.T. January, L.S. Wann, J.S. Alpert, H. Calkins, J.C. Cleveland, J.E. Cigarroa, et al., 2014 AHA/ACC/HRS guideline for the management of patients with atrial fibrillation: a report of the American College of Cardiology/American Heart Association Task Force on practice guidelines and the Heart Rhythm Society, Circulation 130 (2014) 199–267.
[7] W. Zong, R. Mukkamala, R.G. Mark, A methodology for predicting paroxysmal atrial fibrillation based on ecg arrhythmia feature analysis, Comput. Cardiol. 28 (2001) 125–128.
[8] P. Langley, D. Di Bernardo, J. Allen, E. Bowers, F.E. Smith, S. Vecchietti, A. Murray, Can paroxysmal atrial fibrillation be predicted? Comput. Cardiol. 28 (2001) 121–124.
[9] P. Chazal, C. Heneghan, Automated assessment of atrial fibrillation, Comput. Cardiol. 28 (2001) 117–120.
[10] Y.V. Chesnokov, Complexity and spectral analysis of the heart rate variability dynamics for distant prediction of paroxysmal atrial fibrillation with artificial intelligence methods, Artif. Intell. Med. 43 (2) (2008) 151–165.
[11] M. Mohebbi, H. Ghassemian, Prediction of paroxysmal atrial fibrillation based on non-linear analysis and spectrum and bispectrum features of the heart rate variability signal, Comput. Methods Programs Biomed. 105 (1) (2012) 40–49.
[12] K.H. Boon, M. Khalil-Hani, M.B. Malarvili, C.W. Sia, Paroxysmal atrial fibrillation prediction method with shorter HRV sequences, Comput. Methods Programs Biomed. 134 (2016) 187–196.
[13] K.H. Boon, M. Khalil-Hani, M.B. Malarvili, Paroxysmal atrial fibrillation prediction based on HRV analysis and non-dominated sorting genetic algorithm III, Comput. Methods Programs Biomed. 153 (2018) 171–184.
[14] A. Narin, M. Ozer, Y. Isler, Effect of linear and non-linear measurements of heart rate variability in prediction of PAF attack, in: 25th Signal Processing and Communications Applications Conference, SIU, IEEE, 2017.
[15] A. Narin, Y. Isler, M. Ozer, Early prediction of paroxysmal atrial fibrillation using frequency domain measures of heart rate variability, in: Medical Technologies National Congress, IEEE, 2016.
[16] B. Pourbabaee, C. Lucas, Paroxysmal atrial fibrillation diagnosis based on feature extraction and classification, in: Computational Intelligence in Bioinformatics and Computational Biology, CIBCB 2010, IEEE, 2010.
[17] R. Alcaraz, A. Martinez, J.J. Rieta, Role of the P-wave high frequency energy and duration as noninvasive cardiovascular predictors of paroxysmal atrial fibrillation, Comput. Methods Programs Biomed. 119 (2) (2015) 110–119.
[18] A. Martinez, D. Abasolo, R. Alcaraz, J.J. Rieta, Alteration of the P-wave non-linear dynamics near the onset of paroxysmal atrial fibrillation, Med. Eng. Phys. 37 (7) (2015) 692–697.
[19] E. Ros, S. Mota, F.J. Fernandez, F.J. Toro, J.L. Bernier, ECG characterization of paroxysmal atrial fibrillation: parameter extraction and automatic diagnosis algorithm, Comput. Biol. Med. 34 (8) (2004) 679–696.
[20] Physionet AFPDB database, http://www.physionet.org/physiobank/database/afpdb.
[21] J. Park, L. Sangwook, J. Moongu, Atrial fibrillation detection by heart rate variability in poincare plot, Biomed. Eng. Online 38 (2009) 1–12.
[22] Task Force of the European Society of Cardiology and the North American Society of Pacing and Electrophysiology, Heart rate variability: standards of measurement, physiological interpretation, and clinical use, Circulation 93 (1996) 1043–1065.
[23] G. Berntson, J. Bigger, D. Eckberg, P. Grossman, P. Kaufmann, M. Malik, et al., Heart rate variability: origins, methods, and interpretive caveats, Psychophysiology 34 (1997) 623–648.
[24] G.D. Clifford, L. Tarassenko, Quantifying errors in spectral estimates of HRV due to beat replacement and resampling, IEEE Trans. Biomed. Eng. 52 (4) (2005) 630–638.
[25] M.P. Tarvainen, J.P. Niskanen, J.A. Lipponen, P.O. Ranta-aho, P.A. Karjalainen, Kubios HRV—heart rate variability analysis software, Comput. Methods Programs Biomed. 113 (2014) 210–220.
[26] E. Kreyzig, Advanced Engineering Mathematics, seventh ed., Wiley, New York, 1993.
[27] L. Li, K. Li, C.C. Liu, C.Y. Liu, Comparison of detrending methods in spectral analysis of heart rate variability, Res. J. Appl. Sci. Eng. Technol. 3 (9) (2011) 1014–1021.

[28] E.J.M. Weber, P. Molenaar, M.W. Molen, A nonstationarity test for the spectral analysis of physiological time series with an application to respiratory sinus arrhythmia, Psychophysiology 29 (1) (1992) 55–65.
[29] Y. Isler, M. Kuntalp, Combining classical HRV indices with wavelet entropy measures improves to performance in diagnosing congestive heart failure, Comput. Biol. Med. 37 (10) (2007) 1502–1510.
[30] A. Narin, Y. Isler, M. Ozer, Investigating the performance improvement of HRV indices in CHF using feature selection methods based on backward elimination and statistical significance, Comput. Biol. Med. 45 (2014) 72–79.
[31] A. Seyd, P.K. Joseph, J. Jacob, Automated diagnosis of diabetes using heart rate variability signals, J. Med. Syst. 36 (3) (2012) 1935–1941.
[32] M.F. Hilton, R.A. Bates, K.R. Godfrey, M.J. Chappell, R.M. Cayton, Evaluation of frequency and time-frequency spectral analysis of heart rate variability as a diagnostic marker of the sleep apnea syndrome, Med. Biol. Eng. Comput. 37 (1999) 760–769.
[33] B.M. Asl, S.K. Setarehdan, M. Mohebbi, Support vector machine-based arrhythmia classification using reduced features of heart rate variability signal, Artif. Intell. Med. 44 (1) (2008) 51–64.
[34] Y. Isler, Discrimination of systolic and diastolic dysfunctions using multi-layer perceptron in heart rate variability analysis, Comput. Biol. Med. 76 (2016) 113–119.
[35] R.E. Kleiger, P.K. Stein, J.T. Bigger, Heart rate variability: measurement and clinical utility, Ann. Noninv. Electrocardiol. 10 (2005) 88–101.
[36] J.W. Cooley, J.W. Tukey, An algorithm for the machine computation of complex fourier series, Math. Comp. 19 (1965) 297–301.
[37] N.R. Lomb, Least-squares frequency analysis of unequally spaced data, Astrophys. Space Sci. 39 (1976) 447–462.
[38] J.D. Scargle, Studies in astronomical time series analysis II: statistical aspects of spectral analysis of unevenly spaced data, Astrophys. J. 263 (1982) 835–853.
[39] A. Holland, M. Aboy, A novel recursive fourier transform for nonuniform sampled signals: application to heart rate variability spectrum estimation, Med. Biol. Eng. Comput. 47 (7) (2009) 697–707.
[40] P.S. Addison, Wavelet transforms and the ECG: a review, Physiol. Meas. 26 (5) (2005) 155–199.
[41] K. Tanaka, A.R. Hargens, Wavelet packet transform for RR interval variability, Med. Eng. Phys. 26 (4) (2004) 313–319.
[42] I. Guler, E.D. Ubeyli, ECG beat classifier designed by combined neural network model, Pattern Recognit. 38 (2) (2005) 199–208.
[43] C. Orphanidou, I. Drobnjak, Quality assessment of ambulatory ECG using wavelet entropy of the HRV signal, IEEE J. Biomed. Health Inform. 21 (5) (2017) 1216–1223.
[44] O.A. Rosso, S. Blanco, J. Yordanova, V. Kolev, A. Figliola, M. Schurmann, E. Basar, Wavelet entropy: a new tool for analysis of short duration brain electrical signals, J. Neurosci. Methods 105 (2001) 65–75.
[45] R.O. Duda, P.E. Hart, D.G. Stork, Pattern Classification, Second ed., Wiley, New York, 2001.
[46] Y. Saeys, I. Inza, P. Larranaga, A review of feature selection techniques in bioinformatics, Bioinformatics 23 (19) (2007) 2507–2517.
[47] J. Koza, Genetic Programming, MIT Press, Cambridge, MA, 1992.
[48] B. Hickey, C. Heneghan, Screening for paroxysmal atrial fibrillation using atrial premature contractions and spectral measures, Comput. Cardiol. (2002) 217–220.
[49] T. Thong, J. McNames, M. Aboy, B. Goldstein, Prediction of paroxysmal atrial fibrillation by analysis of atrial premature complexes, IEEE Trans. Biomed. Eng. 51 (4) (2004) 561–569.